

Influence of Calcium Carbonate on U(VI) Sorption to Soils

ZUOPING ZHENG,*
TETSU K. TOKUNAGA, AND JIAMIN WAN
Lawrence Berkeley National Laboratory, 1 Cyclotron Road,
Berkeley, California 94720

The high stability of calcium uranyl carbonate complexes in the circumneutral pH range has a strong impact on U(VI) sorption in calcareous soils. To quantify this influence, sorption of U(VI) to soils in the presence of naturally occurring calcium carbonate was investigated by conducting batch experiments in which either U(VI) concentration or solution pH was varied. Two soils containing different calcium carbonate concentrations were selected, one from Oak Ridge, TN, and another from Altamont Pass, CA. The results show that the presence of calcium carbonate in soils strongly affects U(VI) sorption. Higher concentrations of soil calcium carbonate lead to a pronounced suppression of the pH-dependent sorption curve in the neutral pH range because of the formation of a very stable neutral complex of calcium uranyl carbonate in solution. A surface complexation model considering both strong and weak sites for ferrihydrite and ionizable hydroxyl sites for clay minerals was compared with experimental results, and U(VI) binding parameters were reasonably estimated. Fair agreement was found between the model predictions and sorption data, which span a wide range of U(VI) concentrations and pH. The results also show that appropriate solution-to-solid ratios need to be used when measuring distribution coefficients in calcareous soils to avoid complete CaCO_3 dissolution and consequent dilution of calcium uranyl carbonate complexes.

Introduction

Uranium contamination resulting from nuclear energy cycles, weapons processing, interim storage, and disposal practices has been found at a number of United States Department of Energy (DOE) sites (1). To assess the risk of subsurface transport and to facilitate restoration, better understanding of uranium retention, reduction, and immobilization in soils is needed. Under oxidizing geochemical conditions, U(VI) is potentially mobile, with the mobility of soluble U(VI) primarily controlled by sorption (2). In many soil systems, calcite represents an important mineral phase. Despite the well-acknowledged importance of calcite in buffering soil solutions, relatively little work has been reported about the effect of calcite on sorption of U(VI) in soils and sediments. To improve sorption models and describe subsurface transport and fate of U(VI), the role of calcite must be understood under conditions representing natural settings.

Sorption of U(VI) onto geological materials has been studied for decades, and quantitative relations have been provided for a variety of systems (e.g., refs 3–10). Accurately

predicting U(VI) sorption in natural geologic settings, however, remains a challenge because of the large number of mineral phases present in such complex systems. A number of investigations have shown that aqueous U(VI) tends to primarily associate with hydrous iron oxides and clay minerals because of their highly reactive surface areas (11–18). Recently, Barnett et al. (19) demonstrated that similarities in extractable iron concentrations among Hanford, Savannah River, and Oak Ridge Reservation soils led to similar pH-dependent U(VI) sorption, despite significant differences in bulk mineralogy. Their finding underscores the primary importance of iron oxide coatings for U(VI) sorption and the marginal predictive value gained from semiquantitative determination of other common mineral fractions.

Surface complexation models have been used to predict U(VI) sorption in single mineral systems (4, 6, 9, 11, 20–22) because of their satisfactory description of many well-defined sorbing systems, especially with respect to changes in ionic strength and pH (20–22). Applications of surface complexation modeling to U(VI) sorption into soils, however, are less common because of the complexity of natural systems and the incompleteness of thermodynamic database. The principal difficulty in simulating sorption into soils is how to accurately determine the “intrinsic” stability constants of reactions for soil surfaces. The site densities of specific surface functional groups are not tightly constrained, and the compositions of soil solutions are not easily controlled (21). To model sorption into soils, we can apply component additivity (CA) and generalized composite (GC) approaches (21). The CA approach predicts sorption on a complex mineral assemblage by summing the effects of pure, reference minerals or organic phases, whereas the GC approach fits surface complexation equilibria with generic surface functional groups (21). U(VI) sorption to complex solids has been simulated using a CA approach, with varying degrees of success (7, 9, 15). Arnold et al. (16), however, successfully modeled U(VI) sorption onto phyllite by considering iron hydroxide or iron oxyhydroxide as a dominant sorptive phase. In addition, strong sorption of U(VI) onto clay minerals (17, 18) has been reported. Because of the number of mineral phases affecting U(VI) sorption in soils, a GC approach can be useful for predicting U(VI) sorption behavior.

The objectives of this research are (i) to determine distribution coefficients (K_d) for U(VI) sorption on soils in the presence of calcium carbonate as a function of solution pH and U(VI) concentration and (ii) to model the U(VI) sorption process by applying a surface complexation module within PHREEQC 2.0 (23) and comparing modeling predictions and experimental sorption data. A CA approach was taken, combining sorption parameters in the literature with information on acid-extractable Fe and the clay size fraction in two calcareous soils.

Materials and Methods

Materials. Soils used for U(VI) sorption were collected from two locations: Oak Ridge, TN, and Altamont Pass, CA. The Oak Ridge soil was obtained from the background field site used by researchers in the DOE Natural and Accelerated Bioremediation Research (NABIR) Program (24, 25). The Altamont soil was obtained from Altamont Pass (26). Oak Ridge background and Altamont Pass are denoted as ORB and AP, respectively. Soil samples were homogenized and passed through a 2-mm sieve to remove gravel, with the sieved soils then air-dried. The two soils used have relatively high silt and clay percentages (Table 1). A pressure calcimetry method (27) was used to estimate calcium carbonate

* Corresponding author phone: (510)486-6472; fax: (510)486-7797; e-mail: zzuoping@lbl.gov.

TABLE 1. Characterization of the Soils Used in the Experiments

soil particle size analysis ^a	ORB	AP
sand (%)	44.5	10.0
silt (%)	43.0	61.7
clay (%)	12.5	28.3
calcium carbonate (%)	0.1	10.0
extractable iron (mg/g) ^b	3.65	2.36
native organic carbon (ppm) ^a	7.72	0.2
pH (1:1 soil extraction) ^a	5	8

^a From ref 24. ^b This study.

concentrations in the soils. This method is used for quantifying calcite concentrations in soils but is also responsive to a broad range of carbonates. The AP soil has a higher concentration of naturally occurring calcium carbonate than the ORB soil. The ferrihydrite concentrations in the soils were operationally determined by an acid extraction method (28). Surface-area measurements were obtained using the single-point Brunauer–Emmett–Teller approach (Micromeritics, Norcross, GA).

Experiments. Two studies were conducted to evaluate the influence of calcium carbonate on U(VI) sorption into ORB and AP soils. The individual experiments investigated (i) U(VI) concentration-dependent sorption and (ii) pH-dependent U(VI) sorption.

U(VI) Concentration-Dependent Sorption. For these sorption experiments, U(VI) stock solution was prepared by dissolution of certified UO₃ in Milli-Q water. The U(VI) stock solution was diluted to a U(VI) concentration range of 1–30 μ M and then adjusted to pH ~8. The maximum U(VI) concentration used (30 μ M) at pH 8.0, undersaturated with respect to U(VI) minerals, was selected based on thermodynamic calculations with PHREEQC 2.0 (23). For all the solutions, ionic strength was set at 0.01 M with 5 mM KCl and 5 mM NaNO₃. Soil was mixed with U(VI) solution in a ratio of 1:40 (1.00 g of soil in 40 mL of solution) in 50-mL vials at room temperature (23 \pm 1 $^{\circ}$ C) and vented to the atmosphere. All conditions were tested in triplicate. Suspensions were agitated on a shaker for 4 d. Previous kinetic experiments indicated that 4 d was sufficient to reach sorption equilibrium (3, 11, 29), whereas much longer times can lead to removal of some U(VI) from the exchangeable pool (29). After the 4-d equilibration, the final pH of each mixture was measured. The aqueous phase was then separated by centrifugation (4,400 rpm for 30 min) and analyzed for U(VI).

pH-Dependent Sorption. Procedures similar to the U(VI) concentration-dependent sorption were followed, but in this case systematically varying the pH. U(VI) stock solution (~3 mM) was diluted to 5 μ M over the pH range of ~3.0–10.0. The pH was adjusted using 0.1 M nitric acid or 0.1 M sodium hydroxide. The adjustments provided solutions that were within \pm 0.05 pH unit of target values for a minimum of 24 h. After a 4-d period, however, the pH for some batches changed due to calcium carbonate dissolution. A 5-mL suspension was withdrawn for U(VI) concentration analyses after a 4-d period, at which time the pH of the remaining mixtures was readjusted to the initial pH. Successive pH adjustments were periodically monitored and continued until the solution pH was relatively stable. The final U(VI) concentrations and pH values were determined after a total of 8 d. In addition to these samples, operational blanks and reagent blanks were included. Operational blanks consisted of the reaction solutions that were not reacted with the soil sediments. The reagent blank consisted of the distilled water samples used in the preparation of the reaction solutions. Analysis of the operational blanks demonstrated that U(VI) loss to the reaction vial was negligible at the U(VI) concentrations and solution pH range used in this study.

Analysis. U(VI) concentrations were determined by using a kinetic phosphorescence analyzer (model KPA-11, Chem-check Instruments, Richard, WA) with a detection limit of 0.1 ppb.

Degree of U(VI) Sorption. The extent of U(VI) sorption was expressed in terms of the distribution coefficient, which is defined as

$$K_d \text{ (mL/g)} = \frac{S_{\text{uranium(VI)}}}{A_{\text{uranium(VI)}}} \quad (1)$$

where $S_{\text{uranium(VI)}}$ is the U(VI) sorbed on soils (mg/g) and $A_{\text{uranium(VI)}}$ is the U(VI) concentration in aqueous solution (mg/mL). The amounts of U(VI) sorbed were operationally calculated from differences in the measured initial and final U(VI) concentrations in solutions.

Modeling of the U(VI) Aqueous Speciation. The solution chemistry of U(VI) is complicated, with numerous mono- and multinuclear uranium(VI) hydroxide and uranium(VI) carbonate complexes (30). In the presence of atmospheric levels of CO₂, uranium(VI) carbonate complexes (e.g., UO₂(CO₃)₂²⁻, UO₂(CO₃)₃⁴⁻ and Ca₂UO₂(CO₃)₃), which are only weakly sorbed by many mineral forms (3, 9, 31, 32), are the predominant aqueous uranium species at neutral and alkaline pH. In our work, U(VI) speciation was calculated for the solution with a total U(VI) of 10⁻⁶ M in a background electrolyte 0.01 M NaNO₃, equilibrated with and without calcite present. Both cases considered were in equilibrium with the atmosphere (i.e., partial pressure of 10^{-3.5} bar for P_{CO_2}). The distribution of aqueous species was calculated with the program PHREEQC 2.0 using the database from WATEQ4F (23). Data for aqueous uranyl species were supplemented with those from the Nuclear Energy Agency thermodynamic database (33). A neutral calcium uranyl carbonate complex, Ca₂UO₂(CO₃)₃, recently identified in calcium-rich waters (32, 34, 35), was also included. The large value of its stability constant suggests that this complex plays an important role in the environmental chemistry of U(VI). Recently, Brooks et al. (36) found that the presence of this complex greatly inhibits microbial reduction of U(VI) at neutral pH.

The speciation of U(VI) as a function of pH in systems exposed to a P_{CO_2} of 10^{-3.5} bar without calcite or in equilibrium with calcite is shown in Figure 1a,b. As seen for those plots, U(VI) becomes increasingly hydrolyzed and polymerized with increasing pH. Uranium(VI) carbonate complexes become dominant in the high pH range. In the low pH range, UO₂²⁺ is the dominant U(VI) species. However, the neutral U(VI) complex Ca₂UO₂(CO₃)₃ is predominant in the pH range of 7–9 in equilibrium with calcite (Figure 1b).

Modeling of U(VI) Sorption. Surface complexation modeling was used to compare U(VI) partitioning onto well-defined surface sites with measured U(VI) sorption into soils. Spectroscopic evidence has shown the formation of U(VI) binary and ternary complexes on the surface of iron oxides (11, 37). The weak acid-extractable iron was assumed to be ferrihydrite-like and the likely primary sorbing solid phase. The numbers of reactive sites used in the model was set at 0.875 mol of site/mol of extractable Fe, based on Waite et al. (11). The modeling approach follows the two-site model for U(VI) binding to ferrihydrite (38). In the model, two types of surface sites were postulated on the ferrihydrite, a strong site and a weak site. The existence of multiple sites for iron minerals (39, 40) supports this approach. In the two-site approach, the surface protolysis and electrolyte binding reactions for the two site types are assumed to be equal and are given the same log K values. The ratio of weak site to strong site was 476:1 (i.e., 0.21% of the total for the strong sites, 99.79% for the weak sites). The parameters used for ferrihydrite sorption in the two soils are given in Supporting

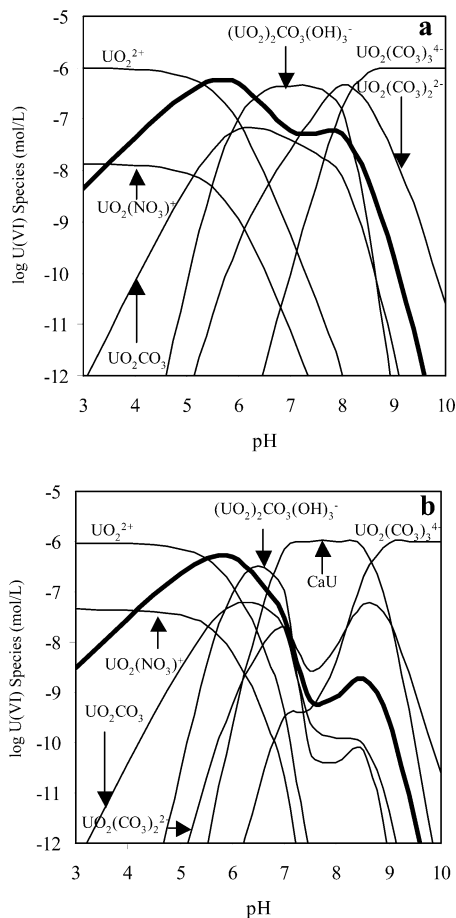


FIGURE 1. Distribution of U(VI) speciation in a 0.01 mol/L NaNO₃ solution with a total dissolved U(VI) of 1.0×10^{-6} mol/L in equilibrium with atmospheric pCO₂ ($10^{-3.5}$ bar) as a function of the solution pH. The heavy curves represent the total concentration of U(VI) hydroxy complexes ($\text{UO}_2(\text{OH})_2$, $\text{UO}_2(\text{OH})_3^-$, $(\text{UO}_2)_2(\text{OH})_2^{2+}$, UO_2OH^+ , and $(\text{UO}_2)_3(\text{OH})_5^+$). CaU refers $\text{Ca}_2\text{UO}_2(\text{CO}_3)_3$. (a) Without calcite. (b) In equilibrium with calcite.

Information Table 1. Surface complexation constants for carbonate sorption on ferrihydrite were derived from the double-layer model by Appelo et al. (41); while the constants for U(VI) sorption onto ferrihydrite were taken from Payne (4). The surface reactions and stability constants for ferrihydrite included in the model are shown in Table 2. U(VI) sorption on clay minerals follows the approach used by Turner et al. (17). In the model, two kinds of surface sites (AlOH and SiOH) were assumed on clay minerals. The surface reactions and stability constants for clay minerals are given in Table 3. Site concentrations for the AlOH and SiOH on clay minerals shown in Supporting Information Table 2 were estimated from Turner et al. (17), through a weighted correction of clay mass fraction. No further adjustments were made for the site concentrations on ferrihydrite and clay minerals.

Results and Discussion

U(VI) Concentration-Dependent Sorption. The distribution coefficients for the two soils investigated at pH 8 as a function of the U(VI) concentrations are presented in Figure 2a,b. As seen here, within the U(VI) concentration range under study, sorption of U(VI) is not linear but rather becomes weaker at higher U(VI) concentrations. Similar results were obtained by others (e.g., refs 4, 9, 29, and 39). Also, under the same conditions, K_d values for the ORB soil are an order of magnitude larger than those measured for the AP soils. This difference is most likely related to the different calcium

TABLE 2. Solution and Surface Reactions Used in the Modeling^a

U(VI) aqueous complexation reactions	log K (I = 0)
$\text{UO}_2^{2+} + \text{H}_2\text{O} \rightarrow \text{UO}_2\text{OH}^+ + \text{H}^+$	-5.20
$\text{UO}_2^{2+} + 2\text{H}_2\text{O} \rightarrow \text{UO}_2(\text{OH})_2 + 2\text{H}^+$	-13.00 ^b
$\text{UO}_2^{2+} + 3\text{H}_2\text{O} \rightarrow \text{UO}_2(\text{OH})_3^- + 3\text{H}^+$	-19.20
$\text{UO}_2^{2+} + 4\text{H}_2\text{O} \rightarrow \text{UO}_2(\text{OH})_4^{2-} + 4\text{H}^+$	-33.00
$2\text{UO}_2^{2+} + \text{H}_2\text{O} \rightarrow (\text{UO}_2)_2(\text{OH})^{3+} + \text{H}^+$	-2.70
$2\text{UO}_2^{2+} + 2\text{H}_2\text{O} \rightarrow (\text{UO}_2)_2(\text{OH})_2^{2+} + 2\text{H}^+$	-5.62
$3\text{UO}_2^{2+} + 4\text{H}_2\text{O} \rightarrow (\text{UO}_2)_3(\text{OH})_4^{2+} + 4\text{H}^+$	-11.90
$3\text{UO}_2^{2+} + 5\text{H}_2\text{O} \rightarrow (\text{UO}_2)_3(\text{OH})_5^+ + 5\text{H}^+$	-15.55
$3\text{UO}_2^{2+} + 7\text{H}_2\text{O} \rightarrow (\text{UO}_2)_3(\text{OH})_7^- + 7\text{H}^+$	-31.00
$4\text{UO}_2^{2+} + 7\text{H}_2\text{O} \rightarrow (\text{UO}_2)_4(\text{OH})_7^+ + 7\text{H}^+$	-21.90
$\text{UO}_2^{2+} + \text{CO}_3^{2-} \rightarrow \text{UO}_2\text{CO}_3$	9.68
$\text{UO}_2^{2+} + 2\text{CO}_3^{2-} \rightarrow \text{UO}_2(\text{CO}_3)_2^{2-}$	16.94
$\text{UO}_2^{2+} + 3\text{CO}_3^{2-} \rightarrow \text{UO}_2(\text{CO}_3)_3^{4-}$	21.60
$3\text{UO}_2^{2+} + 6\text{CO}_3^{2-} \rightarrow (\text{UO}_2)_3(\text{CO}_3)_6^{6-}$	54.00
$2\text{Ca}^{2+} + \text{UO}_2^{2+} + 3\text{CO}_3^{2-} \rightarrow \text{Ca}_2\text{UO}_2(\text{CO}_3)_3$	30.45 ^c
$2\text{UO}_2^{2+} + \text{CO}_3^{2-} + 3\text{H}_2\text{O} \rightarrow (\text{UO}_2)_2\text{CO}_3(\text{OH})_3^- + 3\text{H}^+$	-0.91
$\text{UO}_2^{2+} + \text{NO}_3^- \rightarrow \text{UO}_2\text{NO}_3^+$	0.30
U(VI) surface complexation reactions	log K (I = 0)
$\text{Hfo_wOH} + \text{H}^+ \rightarrow \text{Hfo_wOH}_2^+$	7.29 ^d
$\text{Hfo_sOH} + \text{H}^+ \rightarrow \text{Hfo_sOH}_2^+$	7.29 ^d
$\text{Hfo_wOH} \rightarrow \text{Hfo_wO}^- + \text{H}^+$	-8.93 ^d
$\text{Hfo_sOH} \rightarrow \text{Hfo_sO}^- + \text{H}^+$	-8.93 ^d
$\text{Hfo_wOH} + \text{Ca}^{2+} \rightarrow \text{Hfo_wOCa}^+ + \text{H}^+$	-5.85 ^d
$\text{Hfo_sOH} + \text{Ca}^{2+} \rightarrow \text{Hfo_sOHCa}^{2+}$	4.97 ^d
$\text{Hfo_wOH} + \text{CO}_3^{2-} + \text{H}^+ \rightarrow \text{Hfo_wOCO}_2^- + \text{H}_2\text{O}$	12.78 ^e
$\text{Hfo_sOH} + \text{CO}_3^{2-} + \text{H}^+ \rightarrow \text{Hfo_sOCO}_2^- + \text{H}_2\text{O}$	12.78 ^e
$\text{Hfo_wOH} + \text{CO}_3^{2-} + 2\text{H}^+ \rightarrow \text{Hfo_wOCO}_2\text{H} + \text{H}_2\text{O}$	20.37 ^e
$\text{Hfo_sOH} + \text{CO}_3^{2-} + 2\text{H}^+ \rightarrow \text{Hfo_sOCO}_2\text{H} + \text{H}_2\text{O}$	20.37 ^e
$2\text{Hfo_wOH} + \text{UO}_2^{2+} \rightarrow (\text{Hfo_wO})_2\text{UO}_2 + 2\text{H}^+$	-6.06 ^f
$2\text{Hfo_sOH} + \text{UO}_2^{2+} \rightarrow (\text{Hfo_sO})_2\text{UO}_2 + 2\text{H}^+$	-2.35 ^f
$2\text{Hfo_wOH} + \text{UO}_2^{2+} + \text{CO}_3^{2-} \rightarrow (\text{Hfo_wO})_2\text{UO}_2\text{CO}_3^{2-} + 2\text{H}^+$	-0.24 ^f
$2\text{Hfo_sOH} + \text{UO}_2^{2+} + \text{CO}_3^{2-} \rightarrow (\text{Hfo_sO})_2\text{UO}_2\text{CO}_3^{2-} + 2\text{H}^+$	4.33 ^f

^a Hfo_s and Hfo_w represent strong and weak surface Fe sites, respectively. U(VI) aqueous complexation reactions from ref 33 unless noted otherwise. ^b From ref 50. ^c From ref 34. ^d From ref 23. ^e From ref 41. ^f From ref 4.

TABLE 3. Surface Reactions for Clay Minerals

surface reactions	log K
$\text{SiOH} = \text{SiO}^- + \text{H}^+$	-7.06 ^a
$\text{SiOH} + \text{H}^+ = \text{SiOH}_2^+$	-1.24 ^a
$\text{SiOH} + \text{UO}_2^{2+} = \text{SiOUO}_2^+ + \text{H}^+$	0.146 ^b
$\text{SiOH} + 3\text{UO}_2^{2+} + 5\text{H}_2\text{O} = \text{SiO}(\text{UO}_2)_3(\text{OH})_5 + 6\text{H}^+$	-16.8 ^b
$\text{AlOH} + \text{H}^+ = \text{AlOH}_2^+$	7.6 ^b
$\text{AlOH} = \text{AlO}^- + \text{H}^+$	-10.6 ^b
$\text{AlOH} + \text{UO}_2^{2+} = \text{AlOUO}_2^+ + \text{H}^+$	2.47 ^c
$\text{AlOH} + 3\text{UO}_2^{2+} + 5\text{H}_2\text{O} = \text{AlO}(\text{UO}_2)_3(\text{OH})_5 + 6\text{H}^+$	-17.7 ^c

^a From ref 51. ^b From ref 15. ^c From ref 17.

carbonate concentrations in the two soils. As shown in Figure 1a, weakly sorbed neutral U(VI) complex $\text{Ca}_2\text{UO}_2(\text{CO}_3)_3$ is the dominant U(VI) species at pH 8. The calcium carbonate concentration in the AP soil shown in Table 1 is over 100 times higher than in the ORB soil. It is therefore anticipated that the ORB soil should have higher U(VI) sorption than the

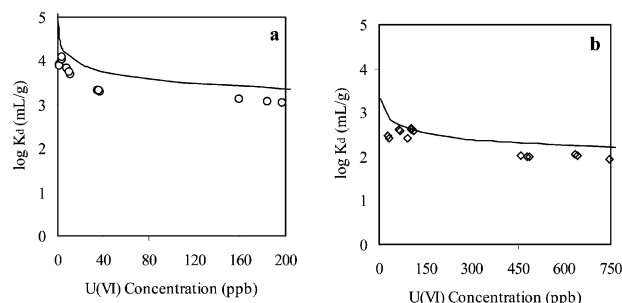


FIGURE 2. Distribution coefficients (K_d) as a function of equilibrium U(VI) concentration for the ORB (a) and AP (b) soils at pH 8. The ionic strength is 0.01 mol/L. The solid curves denote the simulated results for U(VI) sorption on ferrihydrite.

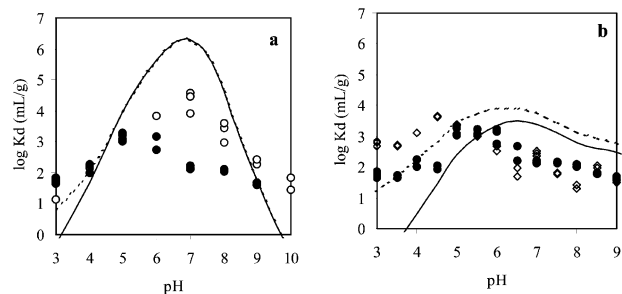


FIGURE 3. Distribution coefficients (K_d) as a function of solution pH for the ORB (a) (\circ), AP (b) (\diamond), and ORB+C (ORB amended with 10% CaCO_3 powder) (\bullet) soils. The initial U(VI) concentration used is 5 μM , and ionic strength is 0.01 mol/L. The solid lines indicate the modeling results considering U(VI) sorption only onto ferrihydrite, whereas dashed curves refer to the modeling results considering U(VI) sorption onto both clay minerals and ferrihydrite.

AP soil because of the stable solution $\text{Ca}_2\text{UO}_2(\text{CO}_3)_3$ complexes. Although the iron oxides, determined by the weak-acid extraction approach (28), are considered as the primary sorptive phase in soils, the difference between the calculated sorptive sites for the two soils based on the iron oxide concentration is slight (Tables 1 and 2). Using a 0.875 mol of sites/mol of Fe as site density for ferrihydrite (11), 65 μmol of sites/g for the ORB soil and 42 μmol of sites/g for the AP soil were obtained, respectively.

pH-Dependent U(VI) Sorption. K_d values as a function of pH for the ORB and AP soils are presented in Figure 3a,b. The pH-dependent U(VI) sorption behavior for the ORB soil shown in Figure 3a is qualitatively consistent with that observed by Barnett et al. (19), although their Oak Ridge soil probably lacked calcium carbonate (since its native pH was 4.7). The maximum K_d occurs in neutral pH range; and K_d decreases under alkaline or acidic conditions. The effect of pH on U(VI) sorption, however, is highly suppressed for the AP soil in the neutral pH range, as indicated by about an order of magnitude lower K_d values, reflecting formation of the neutral U(VI) complex $\text{Ca}_2\text{UO}_2(\text{CO}_3)_3$.

To quantitatively assess the effect of calcium carbonate on U(VI) sorption, U(VI) sorption was conducted by using ORB soils as described previously but amended with 10% CaCO_3 powder, approximately the same amount occurring in the AP soil. Although different from native soil CaCO_3 , this powder solved primarily to ensure that solution Ca^{2+} and HCO_3^- activities remained at or near saturation with respect to calcite. The results practically replicate the U(VI) sorption envelope of the calcareous AP soil for $\text{pH} \geq 5$ (Figure 3b). The large differences between the AP and ORB+ CaCO_3 soils were observed in acidic pH range, but the mechanisms responsible for these differences are not clear. The usual U(VI) sorption envelopes, with maximum K_d observed in neutral pH range (e.g., Figure 3a), were shifted to low pH range with increasing

concentrations of calcium carbonate in soil. In the acidic pH range, U(VI) sorption for the ORB and ORB with added 10% CaCO_3 powder in general is identical (Figure 3a), indicating that the CaCO_3 powder amendment has no effect on U(VI) sorption (in agreement with equilibrium calculations shown in Figure 1a,b). Equilibrium speciation calculations exhibit envelopes of uranium(VI) hydroxy complexes, the dominant species involved in U(VI) sorption, that shift to lower pH with increasing soil calcite. With increasing soil calcite concentrations, $\text{Ca}_2\text{UO}_2(\text{CO}_3)_3$ becomes the predominant U(VI) species in the neutral pH range (data not shown).

A number of pH-dependent U(VI) sorption phenomena have been reported in the literature for a number of systems, including single minerals (e.g., refs 3, 11, 12, and 42–44), mixtures of two minerals (7, 9), and heterogeneous soils (4, 9, 12, 19, 45). U(VI) sorption is strongly dependent on solution pH because of changes in solution speciation as a function of pH, as shown in Figure 1a,b and because of changes in surface species with pH. In the absence of calcite, U(VI) sorption is strong in the neutral pH range where the uranium(VI) hydroxy complexes are important (Figure 1a). In the presence of calcite, however, the more stable neutral U(VI) complex $\text{Ca}_2\text{UO}_2(\text{CO}_3)_3$ is the dominant U(VI) species from pH 7 to pH 9, as shown in Figure 1b. In addition, the decrease in U(VI) sorption at alkaline pH is related to the increased importance of weakly sorbed aqueous uranium(VI) carbonate complexes with increasing pH. In contrast, at acidic pH where the uranyl cation UO_2^{2+} is predominant, UO_2^{2+} sorption is known to be relatively weak.

As reported in several studies, U(VI) sorption on calcite depends on pH, P_{CO_2} , and U(VI) concentrations (46–48). Under slightly alkaline conditions, U(VI) was weakly sorbed as a monolayer (46). Spectroscopic studies (47) suggest that calcite is not likely to be a suitable host for the long-term sequestration of U(VI). Relative to U(VI) sorption onto ferric oxyhydroxides and chlorite, sorption onto calcite is the weakest (48).

The overall capacity of calcite to remove U(VI) from solution is rather limited in the alkaline pH range (45). Thus, the aqueous U(VI) species $\text{Ca}_2\text{UO}_2(\text{CO}_3)_3$ is responsible for decreased U(VI) sorption in the pH range of 7–9 in the presence of calcite. Calcite dissolution in dilute suspensions used in sorption studies can also be important and is addressed in a later section.

Surface Complexation Modeling. Two surface complexation models were used to predict U(VI) sorption. In the first model, ferrihydrite was considered as the only sorptive phase in soils. The surface reactions listed in Table 2, together with site parameters (Supporting Information Table 1), were used in the model to simulate U(VI) sorption. In the second model, both ferrihydrite and clay minerals were considered to contribute to U(VI) sorption in soils. The surface reactions and site concentrations for ferrihydrite used were the same as the first model. Additional surface reactions for the clay minerals used are shown in Table 3. In both models, the calcium carbonate concentrations used for the ORB and AP are 0.25 and 25 mM, respectively. These values represent the equivalent calcium carbonate concentrations in each suspension, based on soil carbonate concentrations (Table 1) and the solution volume to solid mass ratio used in the experiment (40:1). The goodness of fit between the simulated results and experimental data was assessed by the residual root mean square error (RMSE) (49).

Ferrihydrite Model. The K_d values calculated from the sorption data and from the simulated U(VI) sorption on ferrihydrite, as a function of U(VI) concentration (pH 8), compare well (a RMSE in $\log K_d$ of 0.48 was obtained for Figure 2a and of 0.28 was obtained for Figure 2b), supporting ferrihydrite-like complexes as the dominant sorptive phases in both soils. The modeling also indicates that calcium

carbonate concentration in soil strongly affects U(VI) sorption because nearly identical site concentrations but different calcium carbonate concentrations were used for the two soils. In contrast to good matches obtained for sorption isotherms at pH 8, poor fits between prediction of U(VI) sorption onto ferrihydrite and experimental data as a function of pH were observed (data points vs solid lines in Figure 3a,b), as indicated by the larger RMSE values for $\log K_d$ of 1.63 and 1.99 for the solid lines in Figure 3a,b, respectively. The model overestimates sorption by over a factor of 10 in the neutral pH range but underestimates sorption in both acidic and alkaline ranges in the ORB soil. To improve the model prediction, the contributions of other mineral phases to U(VI) sorption should be considered, particularly under alkaline or acidic conditions.

Ferrihydrite + Clay Model. To examine this possibility, we tested a surface complexation model including U(VI) sorption onto clay minerals in the soils with reactions listed in Table 3 together with parameters (Supporting Information Table 2) in addition to U(VI) sorption onto ferrihydrite. The predicted sorption of U(VI) on clay minerals is based on a multiple site-binding model containing edge aluminol and silanol sites developed by Turner et al. (17). The inclusion of these surface reactions (dashed lines in Figure 3a,b) provided a better fit at low pH than obtained by surface reactions on ferrihydrite alone (The smaller RMSE values of 1.48 and 1.35 in $\log K_d$ for the dashed lines in Figure 3a,b). In addition, nearly identical results for sorption as a function of U(VI) concentration (pH 8) are obtained as in Figure 2a,b (data not shown) because U(VI) sorption on clay minerals is fairly weak under alkaline conditions. It is expected that improved fits could be obtained by adding cation-exchange reactions for clay minerals proposed by Turner et al. (17).

Surface complexation modeling provided a fair prediction for U(VI) sorption to soils containing different calcium carbonate concentrations. Since the modeling presented in this paper involves a number of unmeasured parameters and mineral phases, further characterization of the mineralogy, chemistry, and kinetic effects on mineral dissolution and precipitation are needed to improve predictions on U(VI) sorption in subsurface environments.

Environmental and Experimental Implications. Batch experiments and subsequent surface complexation modeling clearly show that calcium carbonate present in natural soils significantly influences pH-dependent U(VI) sorption. In the neutral to slightly alkaline pH range, formation of the neutral U(VI) complex $\text{Ca}_2\text{UO}_2(\text{CO}_3)_3$ appreciably inhibits U(VI) sorption.

The influence of soil CaCO_3 in sustaining U(VI) in stable $\text{Ca}_2\text{UO}_2(\text{CO}_3)_3$ solution complexes has an important consequence for laboratory measurements of U(VI) sorption envelopes and isotherms. Because these measurements are routinely made using very large solution-to-soil ratios, all of the soil calcite originally present could be dissolved. This would significantly lower Ca^{2+} concentrations in solutions and alkalinity relative to levels occurring under field conditions, thus limiting formation of $\text{Ca}_2\text{UO}_2(\text{CO}_3)_3$ complexes and artificially enhancing U(VI) sorption in the neutral to slightly alkaline pH range. The potential magnitude of this artifact becomes apparent when considering the pH-dependent solubility of CaCO_3 at various levels of P_{CO_2} . The general expression provided by Langmuir (30) is

$$\sum \text{Ca}^{2+} = \frac{10^{9.67} [\text{H}^+]^2}{(\gamma_{\text{Ca}^{2+}}) P_{\text{CO}_2}} + \frac{10^{2.96} [\text{H}^+]}{\gamma_{\text{HCO}_3^-}} + 10^{-5.26} \quad (2)$$

where $\sum \text{Ca}^{2+}$ denotes the total concentration of Ca^{2+} in solution (mol L^{-1}), and the γ values are the activity coefficients. Assuming unity for activity coefficients and atmo-

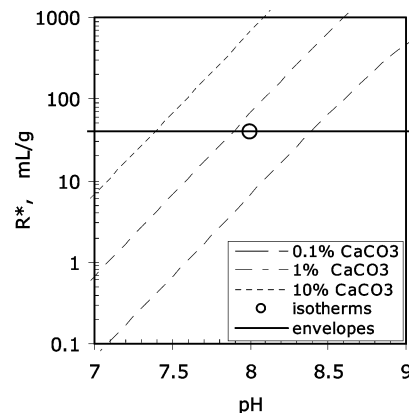


FIGURE 4. Plots of critical solution-to-soil ratios (R^*) vs pH for specific levels of initial soil calcite. When the solution-to-soil ratio is greater than R^* , all of the initial CaCO_3 is dissolved, leaving the solution phase undersaturated with respect to calcite. Also shown is a horizontal line for the solution-to-soil ratio = 40 used in the experiments. These results show that the ORB soil suspensions become calcite undersaturated for $\text{pH} < 8.3$, while the AP suspensions are undersaturated at $\text{pH} < 7.4$.

spheric P_{CO_2} ($10^{-3.5}$ bar), we have

$$\sum \text{Ca}^{2+} = 10^{13.17} [\text{H}^+]^2 + 10^{2.96} [\text{H}^+] + 10^{-5.26} \quad (3)$$

The molar concentration of Ca associated with soil CaCO_3 is equal to the mass fraction of CaCO_3 in soil (denoted as X) times the moles of Ca per mass of CaCO_3 (9.99×10^{-3} mol/g). Combining these relations leads to an estimated upper limit of the solution-to-soil ratio usable without potentially dissolving all of the original soil CaCO_3 . The estimated limiting solution-to-soil ratio is denoted R^* (mL/g) and is given by

$$R^*(\text{pH}) = \frac{9.99X}{\sum \text{Ca}^{2+}} \quad (4)$$

where $\sum \text{Ca}^{2+}$ is given by eq 3. The important pH dependence of this result occurs through the $\sum \text{Ca}^{2+}$ term. Plots of R^* over the neutral to slightly alkaline pH range are shown for several hypothetical soil CaCO_3 concentrations: 0.1, 1, and 10 mass % in Figure 4. For a given soil CaCO_3 concentration, solution-to-soil ratios must be kept less than $R^*(\text{pH})$ to avoid complete dissolution of the native calcite and the resulting artificially high K_d values. This calculation shows that the U(VI) sorption isotherm obtained at pH 8 for the ORB soil is in fact affected by the calcite dissolution artifact, while the AP soil remains safely buffered. In sorption envelope experiments conducted with 40:1 solution-to-soil ratios, the ORB (0.1% CaCO_3) and the AP (10% CaCO_3) soils become calcite-undersaturated at pH values below about 8.3 and 7.4, respectively. If dissolution kinetics are slow enough, these systems will behave as effectively calcite-undersaturated up to higher values of pH. For the ORB soil, the ORB+C envelope (Figure 3a) is in fact the dilution-corrected result. However, since Ca^{2+} concentrations are usually not calcite-controlled at pH much lower than 8, correction for calcite dissolution effects become unnecessary at neutral and acid pH.

These considerations show that detection of diminished U(VI) sorption resulting from formation of calcium uranyl carbonate solution complexes can be easily missed in systems with low calcite concentrations and with high solution-to-soil ratios. In calcareous soils, the calcite content needs to be determined to select solution-to-soil ratios low enough to maintain saturation. Alternatively, higher solution-to-soil ratios can be used when additional CaCO_3 is introduced.

Acknowledgments

This research was funded by the Natural and Accelerated Bioremediation Research (NABIR) program, Biological and Environmental Research (BER), U.S. Department of Energy (Grant DE-AC03-76SF-0098). We thank Jackie Pena (LBNL) for preparing the soils and assisting with U(VI) analyses and Keith Olson (LBNL) for quantifying calcium carbonate in soils. The authors also thank David Watson of the Department of Energy Oak Ridge field site for providing soil samples, Dr. Tianfu Xu (LBNL), Daniel S. Hawkes (LBNL), and three anonymous reviewers for helpful and constructive comments.

Supporting Information Available

Additional information including 2 tables and one brief statement of sensitivity analysis of modeling parameters. This material is available free of charge via the Internet at <http://pubs.acs.org>.

Literature Cited

- (1) Ernest Orlando Lawrence Berkeley National Laboratory. LBNL-49054, 2001.
- (2) Langmuir, D. *Geochim. Cosmochim. Acta* **1978**, *42*, 547–569.
- (3) Hsi, C. D.; Langmuir, D. *Geochim. Cosmochim. Acta* **1985**, *49*, 1931–1941.
- (4) Payne, T. E. Ph.D. Dissertation. University of New South Wales, 1999.
- (5) Pabalan, R. T.; Turner, D. R.; Bertetti, F. P.; Prikryl, I. D. In *Adsorption of Metals by Geomedia*; Jenne, E. A., Ed.; Academic Press: New York, 1998.
- (6) Davis, J. A.; Payne, T. E.; Waite, T. D. *SSSA Spec. Publ.* **2001**, No. 59.
- (7) Prikryl, J. D.; Jain, A.; Turner, D. R.; Pabalan, R. T. *J. Contam. Hydrol.* **2001**, *47*, 241–253.
- (8) Morrison, S. J.; Spangler, R. R.; Tripathi, V. S. *J. Contam. Hydrol.* **1995**, *17*, 333–346.
- (9) Waite, T. D.; Davis, J. A.; Fenton, B. R.; Payne, T. E. *Radiochim. Acta* **2000**, *88*, 687–693.
- (10) Payne, T. E.; Waite, T. D. *Radiochim. Acta* **1991**, *52/53*, 487–493.
- (11) Waite, T. D.; Davis, J. A.; Payne, T. E.; Waychunas, G. A.; Xu, N. *Geochim. Cosmochim. Acta* **1994**, *58*, 5645–5478.
- (12) Duff, M. C.; Amrhein, C. *Soil Sci. Soc. Am. J.* **1996**, *60*, 1393–1400.
- (13) Payne, T. E.; Davis, J. A.; Waite, T. D. *Radiochim. Acta* **1996**, *74*, 239–243.
- (14) Kaplan, D. L.; Gervais, T. L.; Krupka, K. M. *Radiochim. Acta* **1998**, *80*, 201–211.
- (15) McKinley, J. P.; Zachara, J. M.; Smith, S. C.; Turner, G. D. *Clays Clay Miner.* **1995**, *43*, 586–598.
- (16) Arnold, T.; Zorn, T.; Bernhard, G.; Nitsche, H. *Chem. Geol.* **1998**, *151*, 129–141.
- (17) Turner, G. D.; Zachara, J. M.; McKinley, J. P.; Smith, S. C. *Geochim. Cosmochim. Acta* **1996**, *60*, 3399–3414.
- (18) Chisholm-Brause, C.; Conradson, S. D.; Buscher, C. T.; Eller, P. G.; Morris, D. E. *Geochim. Cosmochim. Acta* **1994**, *58*, 3625–3631.
- (19) Barnett, M. O.; Jardine, P. M.; Brooks, S. C. *Environ. Sci. Technol.* **2002**, *36*, 937–942.
- (20) Villalobos, M.; Trotz, M. A.; Leckie, J. O. *Environ. Sci. Technol.* **2001**, *35*, 3849–3856.
- (21) Davis, J. A.; Coston, J. A.; Kent, D. B.; Fuller, C. C. *Environ. Sci. Technol.* **1998**, *32*, 2820–2828.
- (22) Villalobos, M.; Leckie, J. O. *Geochim. Cosmochim. Acta* **2000**, *64*, 3787–3802.
- (23) Parkhurst, D. L.; Appelo, C. A. J. User's Guide to PHREEQC Version 2. *Water Resour. Invest. (U.S. Geol. Surv.)* **1999**, No. 99-4259.
- (24) Pena, J.; Tokunaga, T.; Olson, K.; Herman, D.; Joyner, D.; Hazen, T.; Larsen, J.; Brodie, E.; Firestone, M.; Wan, J. <http://publi-c.ornl.gov/nabirfc>, 2002.
- (25) Driese, S. G.; McKay, L. D.; Penfield, C. P. *J. Sediment. Res.* **2001**, *71*, 843–857.
- (26) United States Department of Agriculture. *Soil Survey: Alameda Area, California*; Series 41; U.S. Government Printing Office: Washington, DC, 1961.
- (27) Sparks, D. L. *Methods of Soil Analyses, Part 3—Chemical Methods*; Soil Science Society of America: Madison, WI, 1996.
- (28) Heron, G.; Grouzet, C.; Bourg, A. C. M.; Christensen, T. H. *Environ. Sci. Technol.* **1994**, *28*, 1698–1705.
- (29) Giammar, D. E.; Hering, J. G. *Environ. Sci. Technol.* **2001**, *35*, 3332–3337.
- (30) Langmuir, D. *Aqueous Environmental Geochemistry*; Prentice Hall: Upper Saddle River, NJ, 1997.
- (31) Lenhart, J. J.; Honeyman, B. D. *Geochim. Cosmochim. Acta* **1999**, *63*, 2891–2901.
- (32) Bernhard, G.; Geipel, G.; Reich, T.; Brendler, V.; Amayri, S.; Nitsche, H. *Radiochim. Acta* **2001**, *89*, 511–518.
- (33) Grenthe, I.; Fuger, J.; Konings, R.; Lemire, R. J.; Muller, A. B.; Wanner, J. *The Chemical Thermodynamics of Uranium*. Elsevier: New York, 1992.
- (34) Bernhard, G.; Geipel, G.; Brendler, V.; Nitsche, H. *Radiochim. Acta* **1996**, *74*, 87–91.
- (35) Kalmykov, S. N.; Choppin, G. R. *Radiochim. Acta* **2000**, *88*, 603–606.
- (36) Brooks, S. C.; Fredrickson, J. K.; Carroll, S. L.; Kennedy, D. W.; Zachara, J. M.; Plymale, A. E.; Kelly, S. D.; Kemner, K. M.; Fendorf, S. *Environ. Sci. Technol.* **2003**, *37*, 1850–1858.
- (37) Bargar, J. R.; Reitmeyer, R.; Davis, J. A. *Environ. Sci. Technol.* **1999**, *33*, 2481–2484.
- (38) Dzombak, D. A.; Morel, F. M. M. *Surface Complexation Modeling: Hydrous Ferric Oxide*; Wiley: New York, 1990.
- (39) Ho, C. H.; Doern, D. C. *Can. J. Chem.* **1985**, *63*, 1100–1104.
- (40) Hiemstra, T.; De Wit, J. C. M.; Van Riemsdijk, W. H. *J. Colloid Interface. Sci.* **1989**, *133*, 105–117.
- (41) Appelo, C. A. J.; Van Der Weiden, M. J. J.; Tournassat, C.; Charlet, L. *Environ. Sci. Technol.* **2002**, *36*, 3096–3103.
- (42) Moyes, L. N.; Parkman, R. H.; Charnock, J. M.; Vaughan, D. J.; Livens, F. R.; Hughes, C. R.; Braithwaite, A. *Environ. Sci. Technol.* **2000**, *34*, 1062–1068.
- (43) Chisholm-Brause, C. J.; Berg, J. M.; Matzner, R. A.; Morris, D. E. *J. Colloid Interface Sci.* **2001**, *233*, 38–49.
- (44) Boulton, K. A.; Cowper, M. M.; Heath, T. G.; Sato, H.; Shibusaki, T.; Yui, M. *J. Contam. Hydrol.* **1998**, *35*, 141–150.
- (45) Gabriel, U.; Gaudet, J. P.; Spadini, L.; Charlet, L. *Chem. Geol.* **1998**, *151*, 107–128.
- (46) Carroll, S. A.; Bruno, J. *Radiochim. Acta* **1990**, *52/53*, 187–192.
- (47) Reeder, R. J.; Nugent, M.; Lamble, G. M.; Drew Tait, C.; Morris, D. E. *Environ. Sci. Technol.* **2000**, *34*, 638–644.
- (48) Milton, G. M.; Brown, R. M. *Can. J. Earth Sci.* **1987**, *24*, 1321.
- (49) Kinniburgh, D. G. *Environ. Sci. Technol.* **1986**, *20*, 895–904.
- (50) Fuger, J. *Radiochim. Acta* **1992**, *58/59*, 81–91.
- (51) Sverjensky, D. A.; Sahai, N. *Geochim. Cosmochim. Acta* **1996**, *60*, 3773–3798.

Received for review May 29, 2003. Revised manuscript received September 19, 2003. Accepted September 26, 2003.

ES0304897